Experimental and numerical study on a sleeping thermal manikin in a mixed ventilation system room

Pan Dong-mei[a], Xia Liang[b], Chan Ming-yin[a*], Deng Shi-ming[a]
[a]Department of Building Services Engineering, the Hong Kong Polytechnic University, Hong Kong
[b]Faculty of Science and Engineering, University of Nottingham, Ningbo, China

ABSTRACT
This paper reports an experimental and numerical study on a sleeping thermal manikin in a room equipped with a mixed ventilation system. In the experimental work, heat loss from the sleeping thermal manikin was measured under different conditions. The supply air temperature was in a range of 20°C to 27.5°C. Apart from the heat loss of the sleeping thermal manikin, the velocity distributions and temperature distributions were also measured in the experiments for subsequent analysis. A numerical model was developed to predict the heat loss from the sleeping thermal manikin. The numerical model was then validated by the experimental results. The results show that thermal comfort levels can be predicted by using a computational fluid dynamic (CFD) model with a high degree of agreement.

Keywords: Computational Fluid Dynamics (CFD); Mixed ventilation system; Sleeping Computational Thermal Manikin (SCTM); Numerical study

1. INTRODUCTION

Current practices in air conditioning are mainly involving the situations in workplaces or other leisure places, such as shopping malls and restaurants and etc. These may however, not be directly applicable to air conditioning provided for sleeping environments. However, in both tropic and sub-tropic regions, the use of air conditioning is to maintain comfortable indoor thermal environments not only in workplaces during daytime, but also in bedrooms of residences, guestrooms in hotels and wards in hospitals, at night time. Therefore, it becomes necessary to study the thermal environment in an air conditioned sleeping space in order to provide people with a thermally comfortable sleeping environment at low energy consumption.

A human being spends approximately one-third of his / her life in sleep. Sleep is not simply a state of rest, but has its own specific and positive functions [1]. Sleep can help people overcome tiredness, and is very important to one's health. In decades, numerous medical researchers have made investigations on various factors related to sleep quality [2-6]. The quality of sleep was mainly determined by two factors: mental-physical factors and bedroom environments. Although the bedroom environments consisted of many factors, including light, noise and thermal environment, the influence of thermal parameters in a sleeping environment on the quality of sleep was gradually acknowledged and documented [7-10]. The last few decades there were a few investigations studying the relationship

between sleeping thermal environment and the quality of sleep. Miyazawa [11] suggested that the range of a thermal neutral temperature was about 22 ± 3°C. Miyazawa further showed that the room air temperature ranged between 11°C and 29°C, the quality of sleep was not significantly affected. Haskell *et al*. [8] reported that there were considerable variations of individual's sensitivity to room air temperature during sleep. It was found that the sleeping patterns of two subjects were similar when the room air temperature was maintained at 29°C. However, these investigations focused solely on the influences of room air temperature. Other factors such as air velocity, air turbulence intensity, radiant temperature of internal walls and the total insulation value of a bedding system could also considerably impact on the quality of sleep, but the acceptable range is bigger. Therefore, it is necessary to embark on studying the effects of other factors both experimentally and computationally rather than solely relying on room air temperature. For experimental studies, thermal manikins were originally introduced at least half a century ago to measure the thermal resistance of clothing. In 1977, Mihira *et al*. [12] developed a thermal manikin not only for clothing insulation measurement, but also for the evaluation of thermal environments. Although an experimental study using a thermal manikin was able to provide detailed information such as air velocity and turbulence intensity, air and wall temperatures, and etc., it could be rather costly and time-consuming. Hence, a growing number of Computational Thermal Manikins (CTMs) have been proposed for the purpose of identifying and evaluating parameters that were either very expensive or very difficult to be experimentally obtained.

A CTM was firstly defined and proposed by Murakami *et al*. [13]. In the study, five CTMs were placed in five different rooms, which were air conditioned with five different air distribution systems. The air flow fields around each CTM and the convective heat transfer between each CTM and its surroundings were numerically investigated and compared. Using the same CTM, the convective and radiant heat transfer, and the moisture transfer between a CTM and its surroundings in a room with a displacement ventilation system was numerically investigated by Murakami *et al*. [14]. The study consisted of two parts: in the first part, a two-node thermoregulation model was employed to simulate the thermoregulatory process and calculate the internal heat transfer inside the CTM; in the second part, the heat and mass transfer between the CTM and its surroundings was numerically modelled. The outputs from the first part, such as sensible heat loss from occupants' skin, Q_t, sweating rate from occupants' skin, m_{sk}, and etc., were used as boundary conditions for the second part. However, the outputs from the second part, such as mean skin temperature, t_{sk}, mean indoor air temperature, t_a, water vapour partial pressure, P_a, and etc., were used as the inputs to the first part. In addition, with the advancement of technology, a CTM with real geometry of a seated female was obtained by scanning through a thermal manikin using laser scanning technique [15]. The CTM was used in a numerical study to assess the effectiveness of a personalized ventilation (PV) system and the related thermal comfort issues. It can be seen that in previous related studies, the main concerns were on the situations where people were awake or where they were in either standing or seated posture. Concerning sleeping environments, the posture for a sleeping person was different from a standing or seated person. The metabolic rate for a sleeping person was 40 W/m^2 which is lower than a standing or seated person, such that the mean skin temperature of a sleeping person in the state of thermal neutrality would be higher. Thirdly, the effects of thermal insulation of clothing were mostly neglected in previous related numerical studies [13-15]. The fact was, however, in a sleeping thermal environment, the total insulation value of a bedding system would play an important role in the thermal neutrality for a sleeping person [16].

This paper reports an experimental and numerical study on a sleeping thermal manikin in a room equipped with a mixed ventilation system. In the experimental work, heat loss from the sleeping thermal manikin was measured under different conditions. The supply air temperature was in a range of 20°C to 27.5°C. Apart from the heat loss of the sleeping thermal manikin, the velocity distributions and temperature distributions were also measured in the experiments for subsequent analysis. A numerical model was developed to predict the heat loss from the sleeping thermal manikin. The numerical model was then validated by the experimental results.

2 EXPERIMENTAL METHODS

2.1 EXPERIMENTAL RIGS

The experiments were conducted in a chamber (Figure 1), and its size was 3,600 (L) mm × 2,500 (D) mm _ 2,500 (H) mm. The thermal manikin was placed with a supine position on a single bed with a dimension of 1,900 (L) mm × 920 (W) mm in the chamber and the bed with mattress was located in the middle of the laboratory. The supply grille was located at the centre-bottom on one side wall, and the return grille was located at the centre-top on the same side wall. The supply air temperature and flow rate can be controlled by a DX conditioning system.

Figure 1. Environmental Chamber

The Thermal Manikin shown in Figure 2, Alex, is divided into 20 independent segments (Left / Right: foot, low leg, front thigh, back thigh, hand, forearm, upper arm, and pelvis, backside, face, crown, chest and back), each with its own temperature sensors, and heating and computer control system to approximately simulate the skin temperature distribution of a human being. In order to correctly simulate the thermal receptors all over the body of a human being, temperature sensing elements are distributed all over the manikin surface. The manikin is heated by the same wiring used for measuring. An individual proportional integral (PI) controller is used to produce the required mean skin temperature in each body segment of the manikin. The mean skin surface temperature, t_{sk}, was an important factor influencing

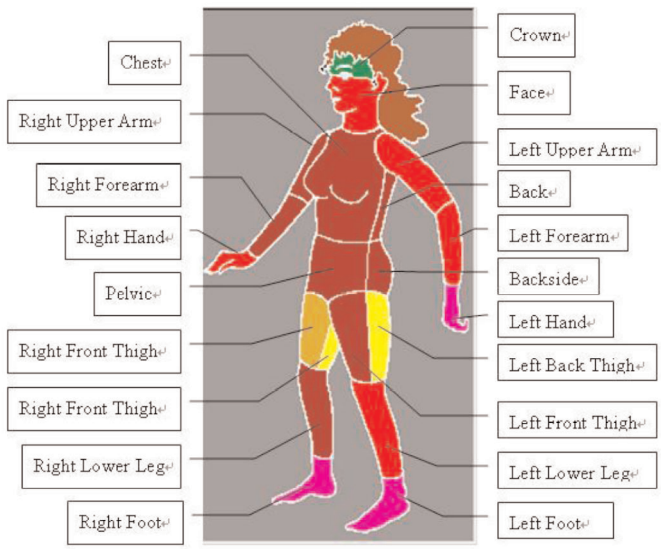

Figure 2. Thermal Manikin

human's thermal sensation. The following linear regression equation, which was proposed as a condition for optimal thermal comfort by Fanger [17], indicated the value of t_{sk}, at which the thermal neutrality may be achieved:

$$t_{sk} = 35.7 - 0.0275(M - W) \tag{1}$$

In the state of thermal neutrality for a sleeping person whose activity level was lower than that for a seated person:

$$M = 40 \tag{2}$$

$$W = 0 \tag{3}$$

Its mean skin temperature would therefore increase to:

$$t_{sk} = 34.6 \tag{4}$$

Therefore, the skin temperature settings were 34.6°C for all body segments. Detailed air velocity and temperature measurements were accomplished by using eight lightweight sensor rigs that allowed a vertical array of sensors to be positioned at the desired measurement heights. At eight locations (as shown in Figure 3) in the chamber, air velocity and temperature were measured at six heights 0.1m, 0.6m, 1.1m and 1.7m. The 0.1m, 0.6m and 1.1m levels correspond to recommended measurement heights for seated subjects as specified by ASHRAE [18]. Temperatures were measured with K-type thermocouples and velocities measured with omnidirectional anemometers having a range of 0~2.5m/s. All sensors were calibrated prior to testing. The measurement accuracy of the anemometer was

estimated to be ±1 % of full scale. In addition, all temperature and velocity data were recorded by two automatic data loggers. During each test, the power input, mean skin temperatures of each segment of the thermal manikin and supply air temperatures were continuously monitored and recorded at an interval of one minute. The mean value of each parameter was calculated based on at least thirty steady-state data.

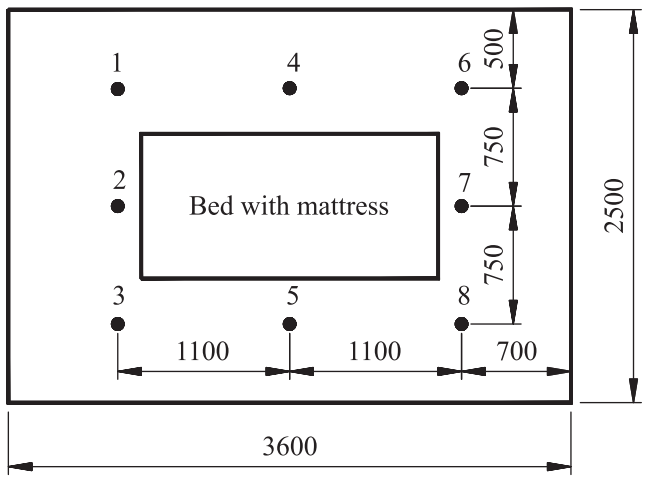

Figure 3. 8 locations of measuring temperatures and associated velocities

The components of a bedding system include bedding, bed and mattress used by occupants during sleep. Two types of summer quilt (Q1 and Q2), and a blanket (B) were used in this study (as shown in Figure 4). Although a variety of mattress types are available; conventional mattress would provide considerably more local insulation than beddings. For all practical purposes, it is assumed that there is no heat loss in steady-state through the body surface in contact with a mattress. However, the firmness of a mattress might affect the amount of body surface area in contact with the mattress, but the resultant variation in insulation is minimal among conventional mattresses [19]. Therefore, only one conventional mattress was used in this study as shown in Figure 5.

Figure 4. Blanket (B), Summer Quilt 2 (Q2), Summer Quilt 1 (Q2)

Figure 5. A conventional Mattress

2.2 EXPERIMENTAL CONDITIONS AND PROCEDURES

The experiments were firstly carried out for a naked thermal manikin under various environmental conditions, and then the thermal manikin was covered by Q1, Q2, B, respectively. When people use bedding, they seldom cover their entire bodies (at least their heads are exposed). People can change their personal insulation by covering and uncovering parts of their bodies with bedding to achieve desired thermal comfort level. To systematically study this effect, McCullough *et al*. [19] developed seventeen different configurations of the body surface coverage by bedding and bed, from the total coverage (100%) to no coverage (23.3% or nude on bed). Three commonly used configurations were selected for experiments. Figure 6 shows examples of experimental conditions and illustrates the placement of bedding on the manikin with different percentage coverage (A_C) of body surface area by bedding and bed indicated for each configuration [20].

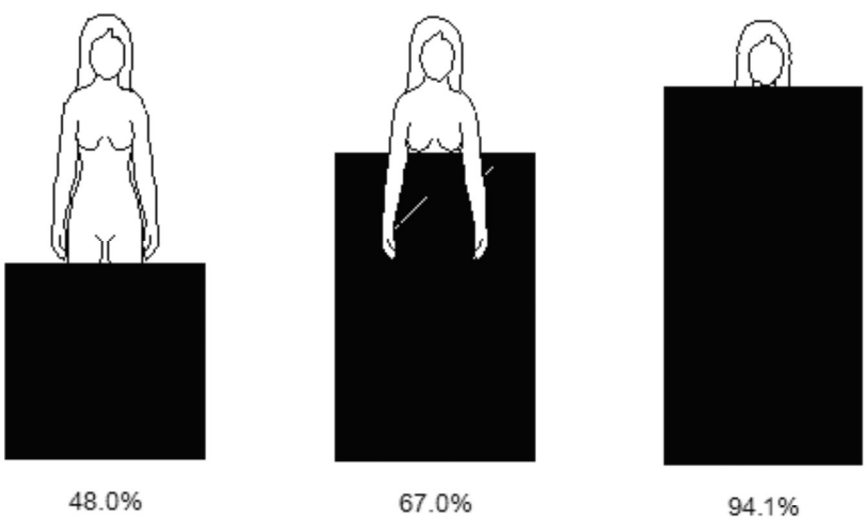

Figure 6. Examples of experimental conditions [20]

3 EXPERIMENTAL RESULTS

3.1 AIR TEMPERATURE AND VELOCITY DISTRIBUTIONS

Figure 7 shows the average air temperatures in four heights under different supply air temperatures. It can be seen that the average air temperature decreased with the increase in height, since the supply grille was located on the top of the one-side wall. The temperature difference was larger with low supply air temperature. However, the temperature differences were not significant among four heights under these conditions. Hence, this mixing ventilation system could create a uniform environment for a sleeping thermal manikin.

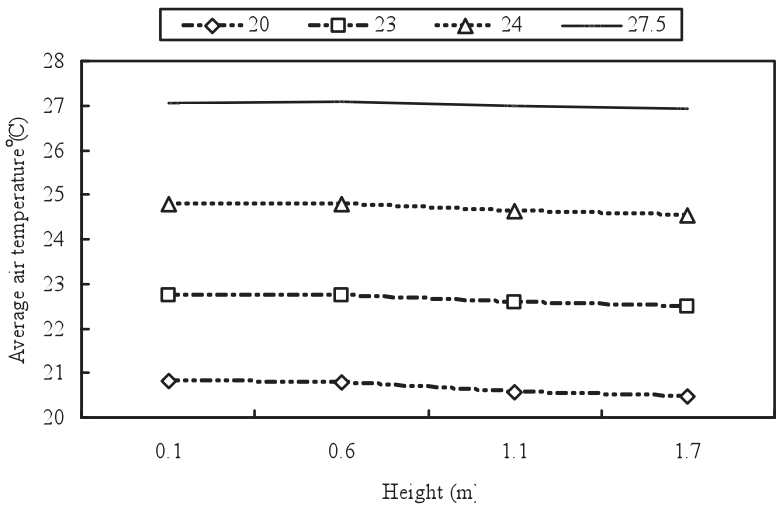

Figure 7. Average air temperatures at 4 heights under different supply air temperatures

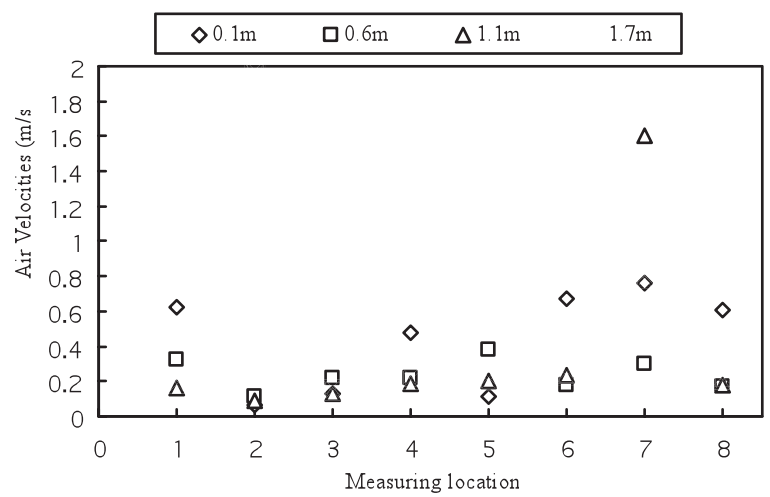

Figure 8. Air velocities at measuring points under supply air velocity 2 m/s

Figure 8 shows the air velocities in all points under supply air velocity at 2 m/s. It can be seen that the air velocities were in the range of to 0 m/s to 0.4 m/s in large parts of points. The air velocities were lower than 0.25 m/s in the height of 0.6 m, which was nearly about the height of the bed with mattress. However, there were a few points where the air velocities were higher, such at the point Location 2 at 1.7m. The point shown in Figure 3 was near to the supply air grille.

3.2 HEAT LOSS FROM A NAKED SLEEPING THERMAL MANIKIN

The heat loss from a naked sleeping thermal manikin may be influenced by various environmental factors, such as air temperatures, wall temperatures, air velocity and etc. Figure 9 shows that heat loss from a naked sleeping thermal manikin under various environmental conditions. It can be seen that the supply air temperature would significantly affect the heat loss. The higher the supply air temperature is, the less the heat loss is. The increase in supply air velocity from 1 m/s to 1.5 m/s resulted in an increase of heat loss 7.3 W/m^2, which was twice of 3.6 $W/m^{2.}$ It was a result of increase in supply air velocity from 1.5 m/s to 2 m/s.

The supply air velocity would also affect the heat loss. The higher the supply air velocity is, the higher the heat loss is. For three supply air velocities, the increase in supply air temperature of 1 K would result in an increase of heat loss 5.27 W/m^2, 5.4 W/m^2 and 5.57 W/m^2, respectively.

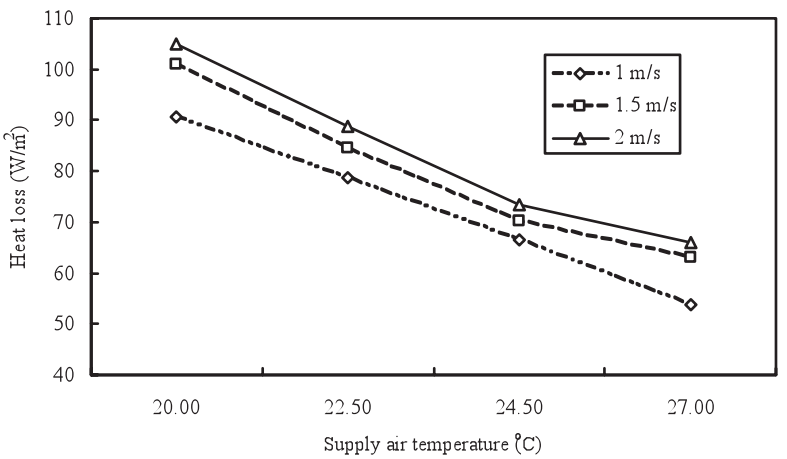

Figure 9. Entire body heat loss from a naked sleeping thermal manikin under various environmental conditions

3.2.1 Heat loss from a covered sleeping thermal manikin

Besides the environmental factors, the total insulation value of a bedding system would play an important role in the heat loss from a covered sleeping thermal manikin [21], in terms of the following two parameters: thermal resistance of a bedding r_b and the percentage coverage of body surface area by bedding and bed A_C [20, 21]. The supply air flow rate and temperature were fixed at 2 m/s and 22°C, respectively in the following experiments, to investigate the effect of these two factors on the heat loss from a covered sleeping thermal manikin.

Figure 10 shows that the heat losses from a covered sleeping thermal manikin with three

different beddings at three different *Ac*. It can be seen that the *Ac* would significantly affect the heat loss from a covered thermal manikin. The higher *Ac* is, the less the heat loss from a covered thermal manikin is. The type of bedding would significantly affect the heat loss from a covered sleeping thermal manikin. However, the difference in heat loss resulted from the bedding became larger, when *Ac* was larger.

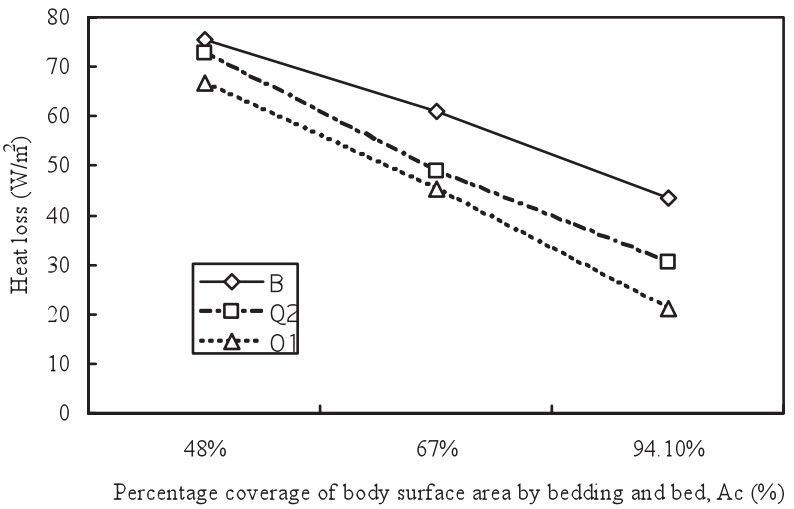

Figure 10. Heat losses from a covered sleeping thermal manikin with three different beddings at three different Ac

4. DEVELOPMENT OF A NUMERICAL MODEL WITH A SIMPLIFIED SLEEPING COMPUTATIONAL THERMAL MANIKIN (SCTM)

4.1 THE NUMERICAL METHOD

4.1.1 Development of a Sleeping Computational Thermal Manikin (SCTM)

The shape of SCTM developed was simplified to a cuboid, measuring at 1,680 mm (W) × 230 mm (D) × 230 mm (H), respectively, as shown in Figure 11. Its total surface area was 1.6514 m^2, which was between the surface area of 1.594 m^2 suggested by Sørensen and Voigt [22], and 1.688 m^2 proposed by Murakami *et al*. [13, 14]. The SCTM was placed on a bed with mattress, whose shape was also simplified to a cuboid, measuring at 1,900 mm (W) × 920 mm (D) × 100 mm (H), respectively, as shown in Figure 11. The percentage coverage of SCTM's surface area by bed with mattress was 23.4%, which was very close to 23.3% proposed by McCullough *et al*. [19].

4.1.2 The air-conditioned space with a mixing ventilation system

The above simplified SCTM was placed in a simulated space installed with a mixing ventilation system as shown in Figure 12, which was created using a commercially available Computational Fluid Dynamics (CFD) software package. The origin of X-Y-Z axes for the simulated air conditioned space was at the left-bottom point of the space. The detailed relative locations of the simplified SCTM, bed with mattress, supply and return grilles and the detailed dimensions of the simulated space are illustrated in Figure 12 and Figure 14, same as the above experimental rigs and conditions. As seen from Figure 12 to Figure 14,

conditioned air was supplied from supply grille located at the centre-top on the left-hand side wall, and returned through the return grille located at the centre-bottom on the same side wall. With the above settings of the simulated space with a mixing ventilation system, and with both the simplified SCTM and the bed with mattress placed inside, it was possible to numerically study the micro-climate around the simplified SCTM.

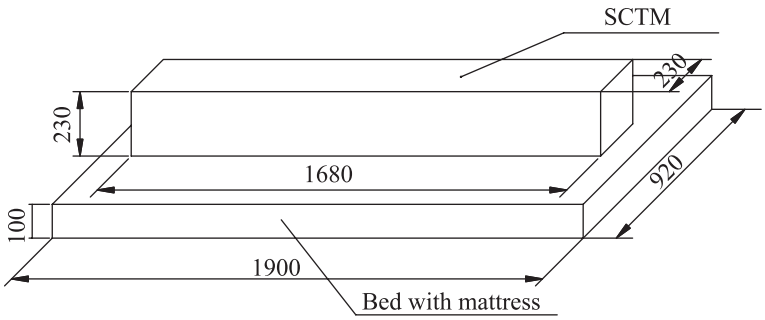

Figure 11. Geometries of the simplified SCTM and bed with mattress

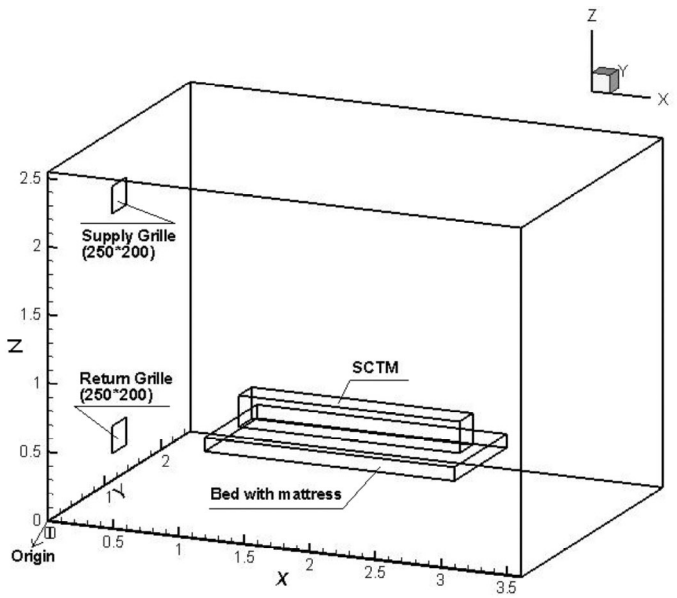

Figure 12. Simplified SCTM placed in a simulated space with a mixing ventilation system

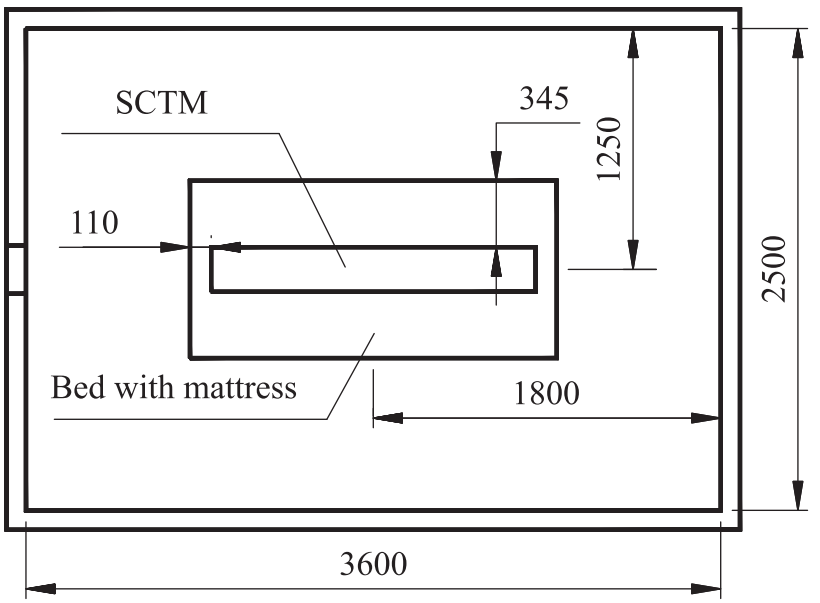

Figure 13. Plan view of the simulated space with a mixing ventilation system

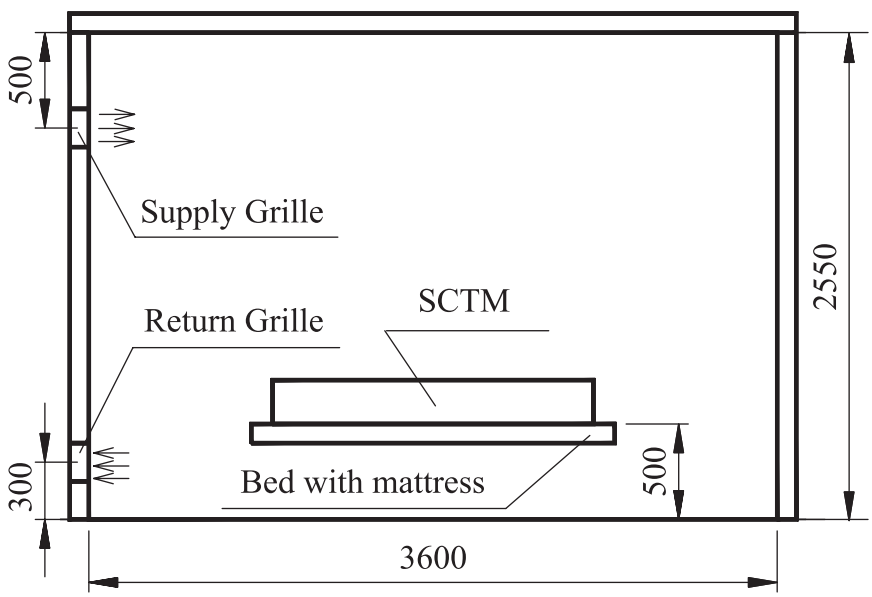

Figure 14. Evaluation view of the simulated space with a mixing ventilation system

4.1.3 Grid generation for numerical study

Given the objective of studying the micro-climate around a sleeping person, the grid generated around the simplified SCTM to be used in this numerical study was therefore carefully selected. The simulated space was divided into two parts as shown in Figure 15: Part A enclosing the simplified SCTM, and Part B for the remaining simulated space. For Part A, the volume boundary layer was firstly created around the simplified SCTM to accurately simulate the viscous boundary and then discretised with unstructured and fine grids, which was able to capture the boundary wall features. For Part B, it was fragmented into structured and coarse girds so as to save computational time. Figure 15 shows the generated grid at y = 1,250 mm plane (Figure 12). The total number of cells generated was 693,528.

On the other hand, the bed with mattress used in this numerical study was regarded as being made of a solid adiabatic material, so that no heat would be lost from a sleeping person through bed with mattress [19].

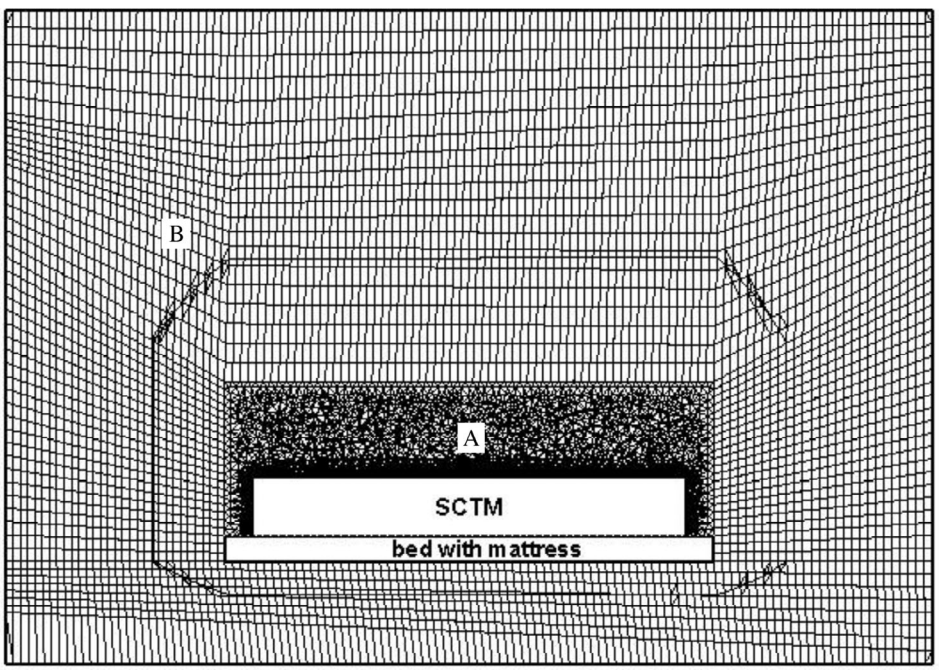

Figure 15. Gird generated in the computational domain (at plane y = 1,250 mm)

4.1.4 Sub-models in the CFD software packages

Various sub-models for simulating the convective, radiant and conduction heat transfer were available in the CFD software package used. The Lauder-Sharma type Low-Reynolds-number k-ε sub-model [23] was used for evaluating the turbulence flow within the simulated space. On the other hand, radiative heat transfer was calculated by using a surface-to-surface (S2S) radiation sub-model, which could account for the radiation exchange in an enclosure of gray-diffuse surfaces. Conduction heat transfer within a thin layer of solid material was evaluated by using the shell conduction sub-model.

4.1.5 Boundary conditions

In this study, the skin temperature of the SCTM was set at a fixed value of 34.6°C, to represent a state of thermal neutrality of a sleeping person. Table 1 shows the detailed boundary conditions used in the numerical study for the simplified SCTM, the wall surfaces and those at the supply and return grilles. When calculating radiant heat transfer, the emissivities of both the SCTM and the room walls, ε_{sk}, ε_{wall}, were set at 0.98 and 0.95, respectively [14, 15].

Table 1. Boundary conditions used in the numerical study

Supply Grille	v=2 m/s; t_{in}=22°C; I = 5 % ; D= 0.22m
Return Grille	Pressure outlet
SCTM	t_{sk}= 34.6°C, ε_{sk}=0.98
Room wall	Adiabatic wall , ε_{wall}=0.95

5. VALIDATION OF THE NUMERICAL MODEL WITH A SIMPLIFIED SCTM

For a naked sleeping thermal manikin, the heat loss was mainly affected by the supply air rate and temperature. To validate the numerical study developed in Section 4, the heat losses were numerically simulated under various environmental conditions, including two different supply air rates: 1.5 m/s and 2m/s, and four different supply air temperature levels.

Figure 16 shows that the comparisons between simulation and experimental heat loss from a nude sleeping thermal manikin. It can be seen that the simulation results agreed well with the experimental values under these environmental conditions, except for one point at 1.5 m/s and 22.5°C. However, the differences between the simulation and experimental results were relatively small.

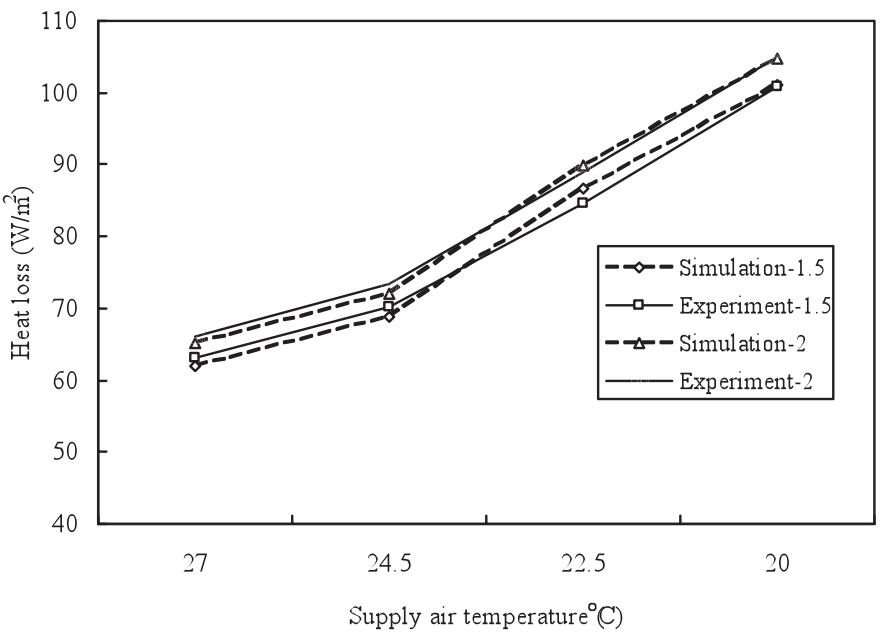

Figure 16. Comparison between the simulation and experimental heat losses from a naked sleeping thermal manikin

The total insulation value of a bedding system would affect the heat loss from a covered sleeping thermal manikin, in terms of the following two parameters: the thermal resistance of bedding r_b and the percentage coverage of body surface area by bedding A_C.

A bedding material had a limited influence on the thermal resistance and the thermal resistance was mainly influenced by its thickness H_{fab} rather than its weight per unit area [24]. In the current studies, different settings of beddings were simulated by adding a shell conduction sub-model, which can evaluate the conduction heat transfer through a thin layer of solid material, such as beddings, to the SCTM.

The thermal resistance of beddings can be evaluated by [25]:

$$r_b = 0.03984 \times H_{fab} \tag{5}$$

Thermal resistances of various beddings were simulated by setting the thickness of the shell conduction at a specific thermal conductivity. Table 3 shows the details of the three beddings [20] used in the experimental study described in Section 2.

Table 2. Measured thickness and evaluated thermal resistances of three beddings [20]

Bedding item	H_{fab} (mm)	r_b (m^2·K/W)
Blanket (B)	3.03	0.121
Summer Quilt 2 (Q1)	7.62	0.304
Summer Quilt 1 (Q2)	15.23	0.607

In addition, for the same bedding, the difference in A_C would also result in difference in R_t. Therefore, the heat losses were numerically simulated under three different beddings and three common used A_C.

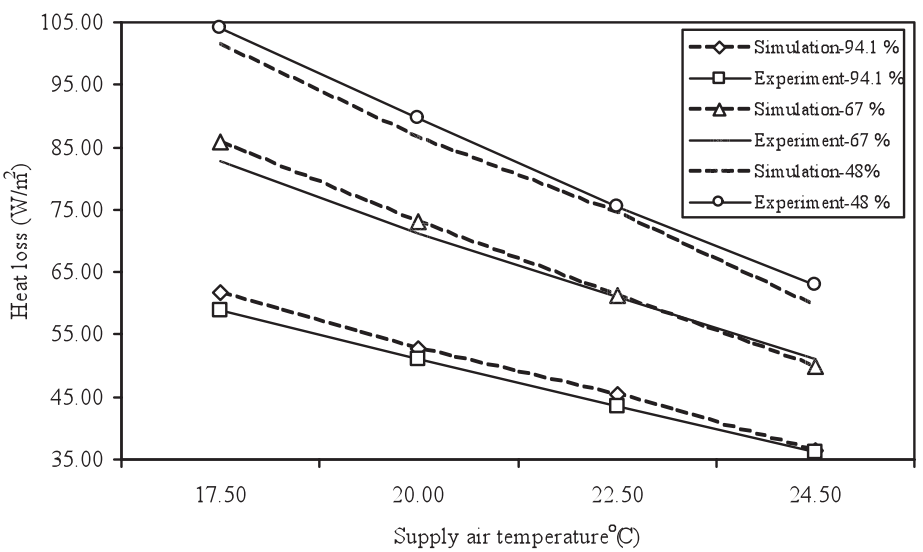

Figure 17. Comparison between the simulation and experimental heat losses for Blanket

Figure 17, 18 and 19 show that the comparisons between the simulation and experimental heat losses for Blanket (B), Summer Quilt 2 (Q2), Summer Quilt 1 (Q1). It can be seen that the simulation results agreed well with the experimental results under those environmental conditions. The differences between the simulation and experimental results were relatively small, and the errors were within ±5%.

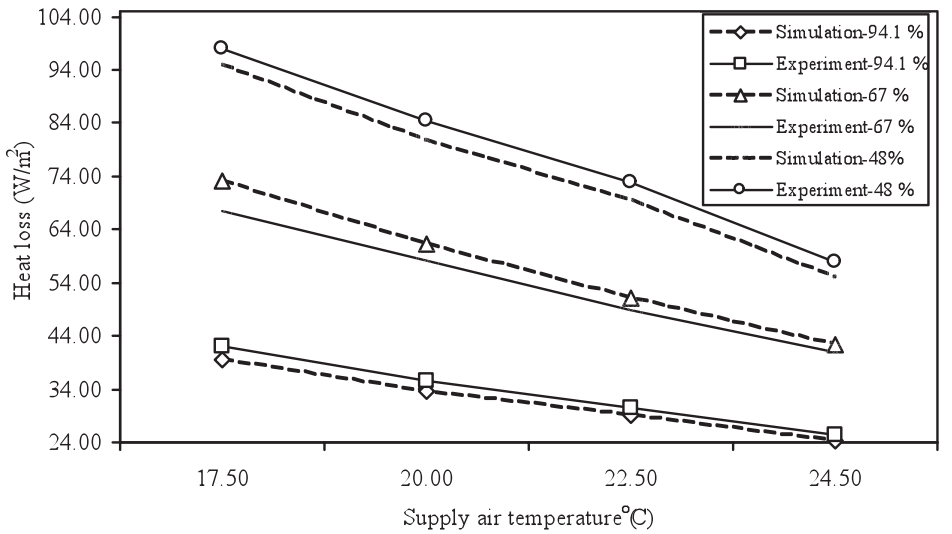

Figure 18. Comparison between the simulation and experimental heat losses for Summer Quilt 2

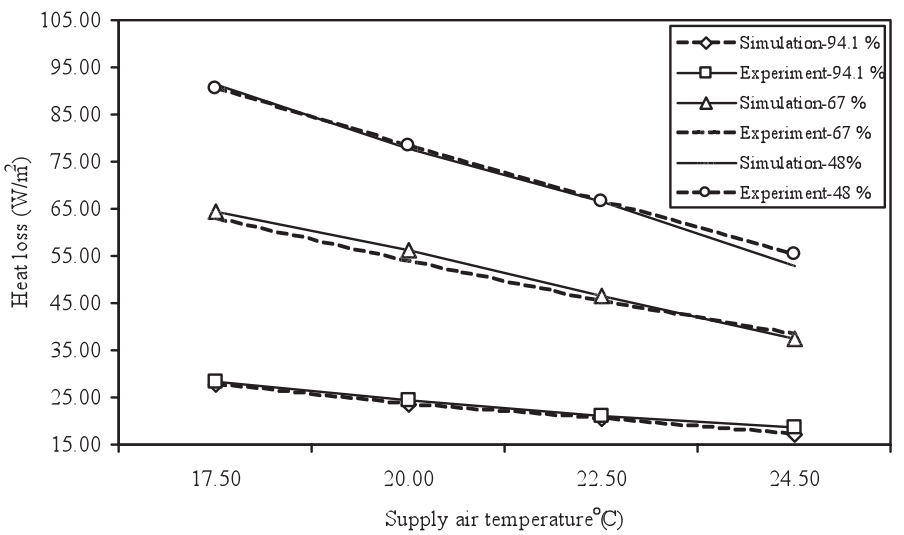

Figure 19. Comparison between the simulation and experimental heat losses for Summer Quilt1

The above analysis suggested that the numerical study with a simplified SCTM developed could predict correctly the micro-climate around, and the heat loss from a sleeping thermal manikin.

5. CONCLUSIONS

A numerical model was developed to predict the heat loss from the sleeping thermal manikin. The numerical model was validated by the experimental results. The results show that thermal comfort levels can be predicted by using a computational fluid dynamic (CFD) model with a high degree of agreement.

ACKNOWLEDGEMENT

The financial support from the Hong Kong Polytechnic University Grant G-YL28 is gratefully acknowledged.

REFERENCE

[1] J.A. Hobson, Sleep. Scientific American Library, A Division of HPHLP, New York ISSN 1040-3213: 1989.

[2] N.G. Cuellar, S.J. Ratcliffe and D. Chien, Effects of depression on sleep quality, fatigue, and sleepiness in persons with restless legs syndrome, *American Psychiatric Nurses Association*, Vol. 12 (5), 2006, pp. 262-271.

[3] K. Sayar, M. Arikan and T. Yontem, Sleep quality in chronic pain patients, *Canadian Journal Psychiatry*, Vol. 49 (9), 2002, pp. 844-848

[4] R. Marc, and M.D. Blackman, Age-related alternations in sleep quality and neuroendocrine function, *The Journal of the American Medical Association*, Vol. 284, n7, 2000, pp. 879-881.

[5] Muzet, A. Environmental noise, sleep and health. *Sleep medicine review*, 2007, Vol. 11, n2, pp. 135-142.

[6] Dauson, D. and Campbell, S. S. Time exposure to bright light improves sleep and alertness during simulated night shifts. *Journal of Sleep Research & Sleep medicine*, 1991, Vol. 14, n6, pp. 511-516.

[7] K. Tsuzuki, K. Okamoto-Mizuno, K. Mizuno and T. Iwaki, Effects of airflow on body temperatures and sleep stages in a warm humid climate, *International Journal of Biometeorology*, Vol. 52, 2008, pp.261-270.

[8] E.H. Haskell, J.W. Palca, J.W. Walker, R.J. Berger and H.C. Heller, The effects of high and low ambient temperatures on human sleep stages, *Electroencephalography and Clinical Neurophysiology*, Vol. 51, 1981, pp. 494-501.

[9] A. Muzet, J.P. Libert and V. Candas, Ambient temperature and human sleep, *Experientia*, Vol. 40 (5), 1984, pp. 425-429.

[10] K. Okamoto-Mizuno, K. Mizuno, S. Michie, A. Maeda and S. Lizuka, Effects of humid heat exposure on human sleep stages and body temperature, *Sleep*, Vol. 22 (6), 1999, pp.767-773.

[11] M. Miyazawa, Seasonal changes of sleep environment at bedtime and on arising, *The proceeding of the 18th symposium on human environment system* (Tokyo 1994), [In Japanese].

[12] K. Mihira, H. Toda and H. Arai, Study on thermal manikin, *Japanese J Human Factor*, Vol. 13 (2), 1977, pp.47-53.

[13] S. Murakami, S. Kato and J. Zeng, Flow and temperature around human person with various room air distribution: CFD study on computational thermal manikin – Part I, *ASHRAE transactions*, Vol.10 (1), 1997, pp.3-15.

[14] S. Murakami, S. Kato and J. Zeng, Combination simulation of airflow, radiation and moisture transport for heat release from a human person, *Building and Environment*, Vol. 35, 2000, pp.489-500.

[15] N.P. Gao, J.L. Niu and H. Zhang, Coupling CFD and human person thermoregulation model for the Assessment of personalized ventilation, *HVAC&R Research*, Vol. 12 (3), 2006, pp.497-518.

[16] Z.P. Lin, and S.M. Deng, A study on the thermal comfort in sleeping environments in the subtropics - Developing a thermal comfort model for sleeping environments, *Building and Environment*, Vol. 43, No. 1, 2008, pp. 70-81.

[17] P.O. Fanger, Thermal Comfort. Danish Technical Press, 1970, Copenhagen.

[18] ASHRAE, ASHRAE handbook of fundamentals, 2009.

[19] E.A. McCullough, P.J. Zbikowski and B.W. Jones, Measurement and prediction of the insulation provided by bedding systems, *ASHRAE Transactions*, Vol. 93 (1), 1987, pp.1055-1068.

[20] Z.P. Lin and S.M. Deng, A study on the thermal comfort in sleeping environments in the subtropics – Measuring the total insulation values for bedding systems commonly used in the subtropics, *Building and Environment*, Vol. 43(5), 2008, pp. 905-916.

[21] D.M. Pan, Z.P. Lin and S.M. Deng, A mathematical model for predicting the total insulation value of a bedding system, *Building and Environment*, Vol. 45(8), 2010, pp.1866-1872.

[22] D.N. Sørensen and L.K. Voigt, Modelling flow and heat transfer around a seated human person by computational dynamics, *Building and Environment*, Vol. 35, 2003, pp. 489-500.

[23] B. E. Lauder and B. I. Sharma, Application of the energy-dissipation model of turbulence to the calculation of flow near a spinning disc, *Letters in Heat and Mass Transfer1*, 1974, pp. 131-138.

[24] ISO 9920 2007. Ergonomics of the thermal environment – Estimation of the thermal resistance and evaporative resistance of a clothing ensemble, 2007.

[25] F. T. Peirce and W. H. Rees, The transmission of heat through textile fabrics – part II. *Journal of the Textile Institute*, Vol. 37(9), 1946, pp. 181-204.